




Short Communication

Design of a GFP reporter for splicing analysis in mammalian cells

Arthur T. Menezes, Helder Y. Nagasse, Hilan R. M. Lopes, Patricia P. Coltri^{*} 

Department of Cell and Developmental Biology, Institute of Biomedical Sciences, University of São Paulo, 05508-000, Brazil

ARTICLE INFO

Keywords:

Pre-mRNA splicing
GFP
Reporter system

ABSTRACT

Eukaryotic genes are formed by exons and introns. Pre-mRNA splicing promotes exon ligation and intron removal and is performed by a specialized macromolecular machinery named spliceosome, composed of five small ribonucleoprotein particles (snRNPs) and more than one hundred proteins. The activity of this complex is highly accurate due to the coordinated activity of its components. Altered splicing has been related to the development of several diseases, including neurodegenerative disorders, such as amyotrophic lateral sclerosis, and different types of cancer. Detailed understanding of splicing regulation in eukaryotic cells can be achieved using splicing reporter systems. We designed a reporter plasmid suitable for splicing analysis in cultured mammalian cells. Our reporter is based on GFP expression, and the splicing outcome can be easily visualized by fluorescence microscopy. We quantified splicing activity in two human cell lines, HEK-293T and MDA-MB-231, confirming its suitability for use in live cells in culture.

List of abbreviations

snRNP – small nuclear ribonucleoproteins
EGFP – enhanced green fluorescent protein
PCR – polymerase chain reaction
pre-mRNA – precursor messenger RNA
cDNA – complementary DNA
RT-PCR – reverse transcriptase – polymerase chain reaction
RNA-seq – RNA sequencing
AdML – adenovirus major late
DMEM / F12 – Dulbecco's modified Eagle's medium/ factor F12
FBS – fetal bovine serum
NaHCO₃ – sodium bicarbonate
PBS – phosphate buffered saline
KH₂PO₄ – monopotassium phosphate
KCl – potassium chloride
NaCl – sodium chloride
mRNA – messenger RNA
Ct – cycle threshold
miRNA – microRNA

1. Introduction

Eukaryotic genes are formed by exons, which remain in the mature RNA sequences, and introns, removed during splicing [1]. Pre-mRNA

splicing relies on recognition of conserved splice sites within the intron and on intron-exon boundaries. Control and efficiency of splicing reactions are essential to gene expression regulation. The process is catalyzed by the spliceosome, a 2 MDa macromolecular complex composed of 5 U-snRNPs (small nuclear ribonucleoproteins U1, U2, U4, U5 and U6) and more than one hundred proteins [2]. The assembly of the spliceosome triggers the two sequential trans-esterification reactions responsible for removing introns and ligating the exons in a mature RNA [3].

Human introns host different non-coding RNAs, including most miRNAs [4]. A great part of these ncRNAs and miRNAs are important for the control of gene expression. As a result, many components related to control of gene expression and abundance of different transcripts are dependent on intron processing. Unbalanced generation of alternative transcripts might be a source for development of pathological conditions, as for example cancer and neurodegenerative diseases [5]. Therefore, understanding the dynamics of splicing activity in different transcripts is essential to predict and control the development of diseases. A major challenge to explore splicing efficiency in a live cell is the difficulty to follow and measure the process [6–8]. First, because transcripts differ in their splicing rates, especially due to differences in splice site sequences and exon-intron base compositions. Secondly, splicing can be largely affected by the cellular environment, which includes the presence of splicing inhibitors and other regulatory proteins [9]. Development of reporter systems will be essential for small compounds

^{*} Corresponding author.

E-mail address: coltri@usp.br (P.P. Coltri).

<https://doi.org/10.1016/j.btre.2025.e00887>

Received 13 December 2024; Received in revised form 7 March 2025; Accepted 13 March 2025

Available online 13 March 2025

2215-017X/© 2025 The Author(s). Published by Elsevier B.V. This is an open access article under the CC BY-NC-ND license (<http://creativecommons.org/licenses/by-nc-nd/4.0/>).

and molecules screening, and might lead to identification of splicing modulators [10]. Real-time RT-PCR has been successfully used to quantify splicing efficiency [11]. This method has shown to be simpler than methods that require autoradiography and cheaper than high-throughput methods, such as RNA-seq, which demands a long workflow for each experimental group tested [12].

In order to understand how splicing regulation can guide the development of diseases, it is important to address its efficiency and regulation in different cell lines [7]. In this sense, the use of a fluorescent gene could be useful to follow RNA processing and splicing outcome. We therefore developed a reporter system based on GFP coding sequence to characterize splicing efficiency in cultured cells. The GFP coding sequence was split into two exons and an intron derived from the AdML gene was inserted between them. Our reporter transcript allows visualization and quantification of splicing reactions by fluorescence microscopy and real-time RT-PCR, enhancing our capacity to analyze gene expression and splicing efficiency in cultured cells.

2. Methods

2.1. Construction of pGFP-spl reporter

The EGFP coding sequence was amplified by PCR using pEGFP vector (Invitrogen) as DNA template in 2 separate fragments, named “exon 1” and “exon 2”. 336 bp “Exon 1” was amplified using primers PC20 (5′ ACGCTGGATCCATGGTGAGCAAGGGCGAGG 3′) and PC21 (5′ GGAGTGAATTCACCTCGGCGGGTCTTG 3′), flanked by BamHI and EcoRI restriction sites. 384 bp “Exon 2” was amplified using primers PC28 (5′ GAAACTGCGGCCGCCACAGGTGAAGTTCGAGGGCGACACCC 3′) and PC29 (5′ GCCGCTTCTAGATTACTGTACAGCTCGTCCATGCC 3′), flanked by NotI and XbaI restriction sites. The 123 bp intron sequence was amplified from the AdML precursor [13], flanked by EcoRI and NotI restriction sites (PC26: 5′ GAAACTGAATTCACCTCCTCTCAAGCGGGC 3′, and PC27: 5′ GAAACTGCGGCCGCAAAAAAGGACAGGGTCAG 3′). “Exon 1”, “exon 2” and the intron products were cloned into pGEM-T-easy vector (Promega), according to manufacturer’s instructions, followed by DNA sequencing. After confirmation of

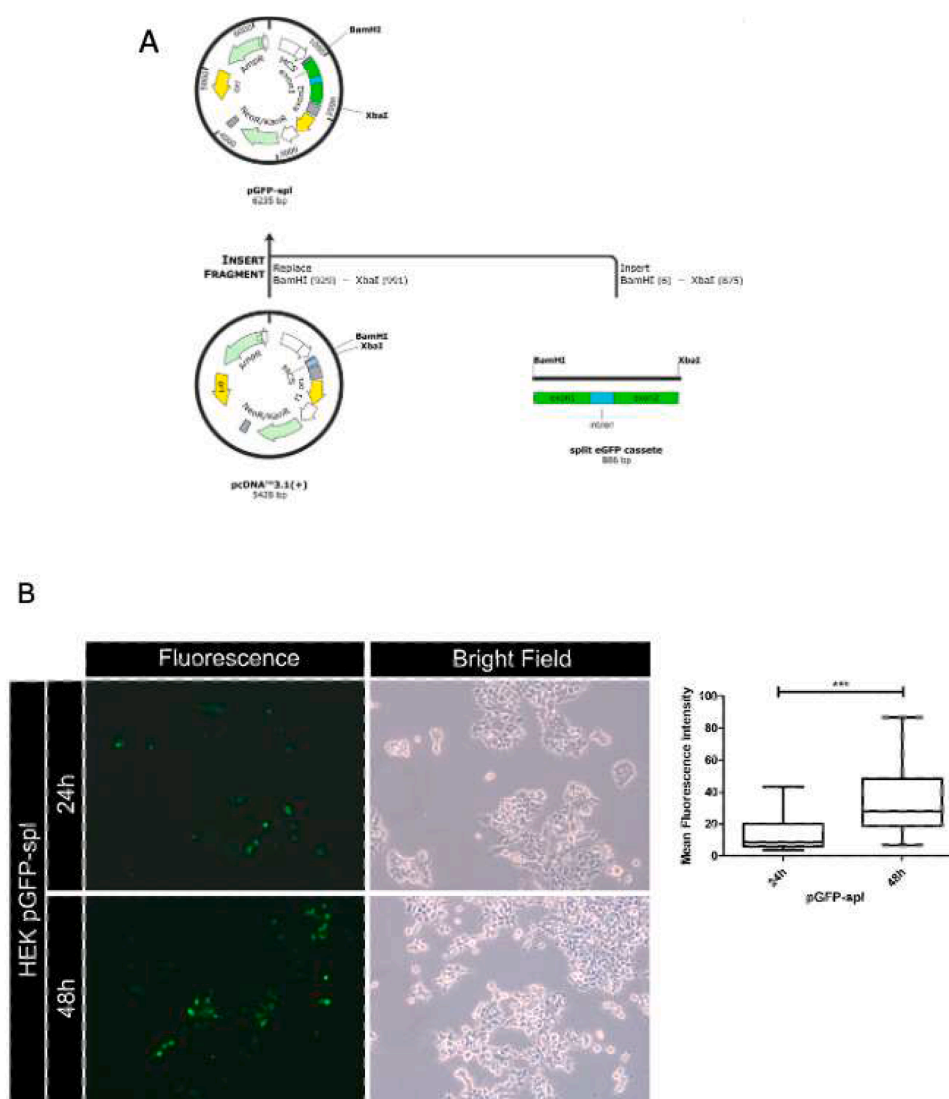


Fig. 1. pGFP-spl plasmid construction and fluorescence analysis of GFP expression in HEK-293T live cells. (A) The generation of pGFP-spl is shown, with the cassette containing GFP exons (green) and the intron (blue) (843 bp). Total length of spliced GFP exons (“mRNA”) is 720 bp, and intron length is 123 bp. (B) Fluorescence after 24 h and 48 h of transfection is shown on the left and bright field is on the right. Magnification 40x. Mean fluorescence intensity quantification from approximately 100 cells are shown on the right-hand side. pGFP-spl mean fluorescence intensity was quantified after 24 h and 48 h of transfection using Fiji software. Statistical analysis was performed by unpaired T-test (GraphPad Prism 8.0.2). ***p < 0.001. Further fields are shown in Supplementary Figure 2 and raw images are available at <https://github.com/PColtri/Menezes2025/>.

sequence integrity, the “exon 1 – intron – exon 2” cassette was subcloned into pcDNA 3.1(+) vector (Invitrogen), using BamHI and XbaI enzymes resulting in the splicing reporter plasmid pGFP-spl (Fig. 1A and Supplementary Figure 1). Importantly, both pEGFP and pcDNA 3.1(+) vectors carry the mammalian CMV promoter and ampicillin resistance marker.

2.2. Cell culture and transfection

HEK-293T and MDA-MB-231 cell lines were cultivated in 100 mm plates in 10 mL of DMEM high glucose (Thermo) with 10 % FBS and 3.7 g / L NaHCO₃ in a humidified, controlled atmosphere incubator (5.0 % CO₂) at 37 °C. Transfections were performed using Lipofectamine 2000 (Thermo), according to manufacturer's instructions, when cells reached 70–80 % confluence. 1.5 µg of plasmid DNA was used to transfect the cells.

2.3. Cell analysis by fluorescence microscopy

Cells were analyzed by fluorescence microscopy to check for GFP expression 24 h and 48 h after transfection. A fluorescence microscope (Axio Vert. A1 Zeiss) at 40x magnification was used. Untransfected cells were used as controls. The photos were analyzed using Fiji software (version 2.14.0) to quantify the mean fluorescence intensity [14]. Approximately 100 cells for pGFP-spl were quantified from three different photos (Fig. 1 and Supplementary Figure 2). Image thresholds were normalized and fluorescence intensities for each group were measured and analyzed. Image background was normalized as previously described [14].

2.4. RNA analysis and real-time RT-PCR

Cells were collected and washed in a PBS buffer (3.2 mM Na₂HPO₄, 0.5 mM KH₂PO₄, 1.3 mM KCl, 135 mM NaCl [pH 7.4]). Total RNA was extracted using Trizol (Thermo), according to the manufacturer's

instructions. After Trizol extraction, samples were precipitated using 3 M sodium acetate pH 5.2 and 100 % ethanol. RNA samples were used for cDNA synthesis using the Superscript kit (Thermo) and random primers. 100 ng of these cDNAs were analyzed by PCR, and real-time RT-PCR (RT-qPCR). PCR reactions were performed with a hot start at 94 °C for 5 min; then 35 cycles as follows: 94 °C for 30 s; 59 °C for 30 s; 72 °C for 30 s. A final extension at 72 °C for 7 min and then hold at 4 °C. Total RNA was detected using the primers spanning exons 1 (forward) and 2 (reverse) (PC155: 5' GACGACGGCAACTACAAGAC 3' and PC156: 5' GATGCCCTTCAGCTCGATGC 3') (represented in Fig. 2A). Importantly, the ‘total RNA’ refers to the amplification of both pre-mRNA and mRNA, as the primer pair PC155/PC156 can amplify both RNA forms. Mature RNA was detected upon amplification using forward ‘exon junction’ and reverse ‘exon 2’ pair of primers (PC157: 5' GCGCCGAGGTGAAGTTC 3' and PC156: 5' GATGCCCTTCAGCTCGATGC 3'). RT-qPCR reactions were prepared using SYBR Green® reagent (Thermo) and specific primers. For GFP pre-mRNA quantification, the primers amplify a region between the intron (forward, PC387: 5' GTGCTGACCTGTCCCTTTT 3') and the exon 2 (reverse, PC388: 5' TTCTGCTGTGCGCCATGAT 3'). For GFP mRNA quantification, primers PC157 and PC156 were used as indicated above. β-actin primers were used for normalization (primers PC168: 5' ACCTTCTACAATGAGCTGCG 3' and PC169: 5' CCTGGATAGCAACGTACATGG 3').

Splicing efficiency was calculated by the fold change of mRNAs using pEGFP as standard, after β-actin normalization, based on previously described methods [15], and considering the variation between the RT-qPCR technical replicas. Splicing efficiency of time-course experiments were calculated using the same procedure but using the 1 h time point as standard.

2.5. Statistical analysis

Fluorescence image intensities and RT-qPCR data were subjected to statistical analysis using two-tailed unpaired T-test or One-way ANOVA with Tukey's post-hoc (GraphPad Prism 8.0.2).

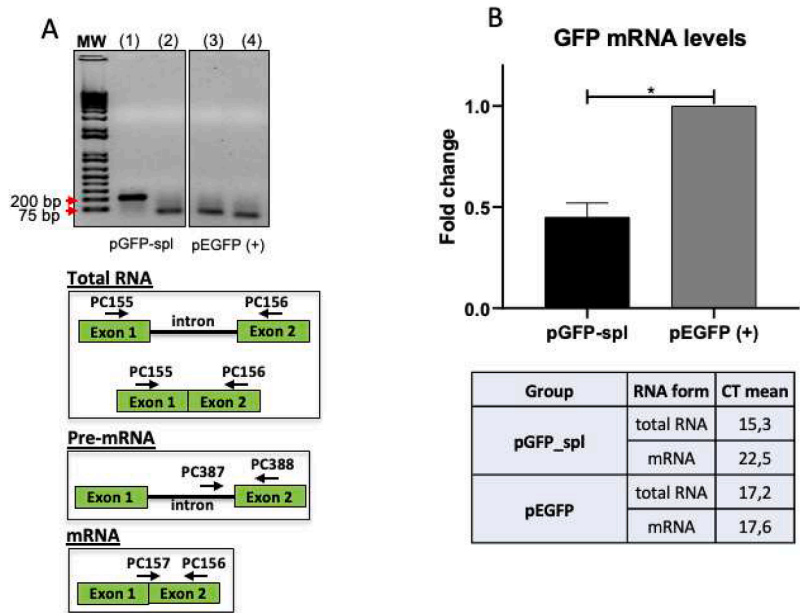


Fig. 2. PCR and RT-qPCR analysis of splicing. HEK-293T cells were transfected with pGFP-spl and pEGFP (Invitrogen) as a positive control. (A) Electrophoresis of PCR products. PCR reactions were performed using cDNA as template and primers to detect the transcripts corresponding to total RNA (odd lanes, PC155/PC156) and mRNA (even lanes, PC157/PC156). The schemes at the bottom show the primer pairs annealing to amplify total RNA, pre-mRNA and mRNA. Red arrowheads on the left point to reference size bands for comparison. MW: Molecular weight ladder 1 kb (Thermo). (B) Graph showing fold change in mRNA levels after normalization with β-actin and using pEGFP as standard. pGFP-spl and pEGFP (positive control) are shown. Standard deviations were calculated after two technical replicates. Statistical analysis was performed by unpaired T-test (GraphPad Prism 8.0.2). *p < 0.01. In the lower part of the figure, the raw Ct mean for each sample and with both sets of primers are shown.

3. Results and discussion

pGFP-spl was generated upon ligation of EGFP sequence divided in two exons and AdML intron (Fig. 1A). HEK-293T cells transfected with pGFP-spl were analyzed by fluorescence microscopy after 24 h and 48 h (Fig. 1B). We observed EGFP expression through the fluorescence signal in the transfected cells, confirming both the transfection and generation of mature mRNA occurred. Upon transfection, transcription of EGFP pre-mRNA led to generation of a mature transcript followed by translation and folding of GFP, which resulted in the fluorescence observed. Fluorescent and bioluminescent proteins are widely used as expression reporters in mammalian cells [16–18]. We noticed a higher fluorescence intensity after 48 h of transfection, indicating production of GFP increased over time. It is possible that the presence of the intron increased stability of the pre-mRNA generated by the reporter, leading to a continuous increase on GFP translation [19]. These results confirmed our reporter was successfully spliced and resulted in mature GFP protein.

Generation of mature GFP mRNA from the reporter plasmid was confirmed by qualitative PCR and by RT-qPCR (Fig. 2). To assess splicing, we used a set of three different pairs of primers to detect mRNA, pre-mRNA and total RNA (as described in the Methods section). Importantly, “total RNA” refers to products amplified from both pre-mRNA and mRNA molecules, once primers are complementary to exon 1 and exon 2, “pre-mRNA” refers to amplification of pre-mRNA products only, and “mRNA” refers to products derived from mature mRNAs only (Fig. 2A, lower panel).

HEK-293T cells were analyzed 48 h post-transfection. The spliceosome machinery was able to process GFP pre-mRNA transcribed from pGFP-spl plasmid, since both pre-mRNA and mRNA were observed (Fig. 2A). Odd lanes show PCR products using the primers for total GFP RNA amplification, and even lanes show PCR products for GFP mRNA. The band in lane 1 is possibly the result of amplification of the pre-mRNA and residual plasmid DNA, since these primers can anneal to both templates (Supplementary Figure 3). But a lower band corresponding to mRNA would also be expected, since this pair of primers also amplifies mRNA. It is possible that during the PCR reaction, cDNAs corresponding to pre-mRNA and mRNA competed for primer binding and more pre-mRNA and residual plasmid DNA are in the sample, explaining the higher intensity of this band. The GFP mRNA was also present in the positive control (Fig. 2A, lanes 3 and 4). pGFP-spl transfected cells still retain unspliced pre-mRNA, as one would reasonably expect considering pre-mRNA splicing reactions dynamics [20].

The splicing efficiency observed for pGFP-spl was determined by mRNA and total RNA quantification through RT-qPCR. PC155/PC156 pair was used to assess ‘total RNA’ and PC157/PC156 was used to assess ‘mRNA’. Raw Ct numbers of both amplifications are shown in the box below Fig. 2B. To calculate the fold change in the amount of mRNA generated, Ct’s from ‘mature RNA’ pair of primers were normalized by β -actin levels and pEGFP was used as the positive control (Fig. 2B). pGFP-spl showed 0.4-fold change in mRNA, indicating lower GFP mRNA levels compared with the pEGFP positive control. Still, the presence of mRNA confirms the reporter pGFP-spl was spliced. The lower amount of GFP mRNA generated from the reporter is expected due to: (1) our assay used a commercial plasmid as positive control, containing the EGFP sequence without introns, which means that all transcribed molecules generate EGFP mRNA; (2) pGFP-spl does not integrate in the genome. Transcription and subsequent splicing depend on the cell machinery, and only a part of pre-mRNA will be processed, as observed by *in vitro* assays [21]. Next, we wondered whether the splicing rate could change over a period after transfection. Since our reporter is derived from an episomal plasmid, we reasoned longer periods of incubation after transfection could increase the processing rate. To address when mRNA was processed after transfection, we performed a time-course experiment.

The time-course experiment was performed by collecting HEK-293T

and MDA-MB-231 cells after 1, 3 and 24 h of pGFP-spl transfection. Since the GFP fluorescence intensity was high at 24 h, as observed in Fig. 1, we used this as the last time point for mRNA analysis. Splicing efficiency was calculated using time point 1 h as the standard level. Our results with HEK-293T cells showed that mRNA levels increase after transfection, reaching ~6-fold change in 24 h, in comparison to the levels observed after 1 h (Fig. 3A). Following transfection, pre-mRNA shows a peak after 3 h but reduces to <0.5-fold change after 24 h, indicating most of it has been processed into mRNA (mGFP) during this interval (Fig. 3B). A similar profile is observed in MDA-MB-231 cell line, with a pre-mRNA peak after 3 h, which reduces after 24 h (Fig. 3D) concomitant with mRNA increase, reaching ~2.5-fold change in 24 h (Fig. 3C). This is expected because upon transfection, EGFP pre-mRNA is generated by transcription of the reporter plasmid, followed by processing and splicing, leading to generation of mature EGFP mRNA. The time-course analysis revealed different cell lines have similar GFP production upon the reporter plasmids transfection, but HEK-293T generated slightly more mRNA than MDA-MB-231. Nevertheless, both can generate mRNA from the pGFP-spl reporter.

Fluorescence-based plasmids have been used to study splicing events under different contexts [7]. Different approaches have been used to develop reporter systems, including single and dual-gene reporters, the use of luciferase [22,23,8,10], β -galactosidase, radionuclides, and ribozymes [7]. To analyze the splicing efficiency, our reporter consists of a single-intron mini-gene system that offers a new tool to explore splicing in cultured cells, allowing for characterization of effects that stimulate or inhibit splicing in a straightforward manner. Our splicing reporter system allows for a rapid quantification of GFP splicing outcome in cell cultures using a fluorescence microscope, without the need to collect and process cells. In addition, the amount of GFP produced can also be accessed through PCR and/or western blot, resulting in an easy and cheaper method to analyze splicing. At this stage of analysis, procedures such as collecting cells and preparing them for flow cytometry would not be necessary. In addition, our reporter allows the inclusion of regulatory sequences in the intron, as for example miRNAs and other types of non-coding RNAs. This can be especially important to analyze how transcripts with different exon/intron compositions are processed under different conditions.

Previous works measured alternative splicing using fluorescence-based plasmids. A system based on the interrupted mCherry gene was used to analyze alternative splicing [24]. Depending on the alternative splicing pattern, the sequence that interrupts mCherry gene could be removed or skipped, therefore allowing visualization of alternative splicing through a fluorescence microscope. These reporters can be extremely useful in high throughput screenings to identify compounds or small molecules capable of regulating or blocking splicing [25,26]. Identification of alternative splice sites in mouse VEGF-A transcript was carried out using a splicing sensitive fluorescent reporter, offering new possibilities to detect specific tissue splicing patterns and possible therapies [27].

Our reporter system could be used for alternative splicing studies if additional splice sites were included in the intron. The presence of an additional splice-site (or sites) could recruit the machinery and, if inclusion of intron occurs in the mRNA, the entire EGFP sequence would not be reconstituted, therefore not generating fluorescence. Also, another intron-exon cassette could be included on the 3'-end of the current reporter, for example including a tag on this exon. Splicing of this modified reporter would allow for visualization of a GFP-tagged protein. Future studies should explore the inclusion of other sequences, such as non-coding RNAs or miRNAs within the intron, which could improve studies of splicing regulation upon specific cellular conditions. Some other possible applications would be the study of different elements that affect splicing dynamics, such as the use of drugs targeting the spliceosome.

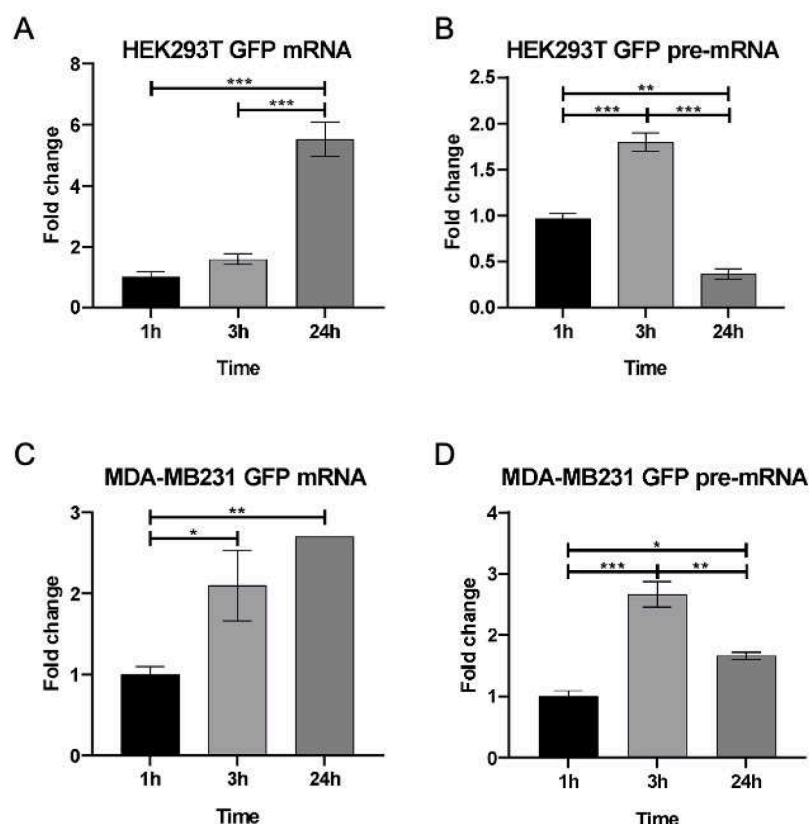


Fig. 3. Time-course analysis of splicing reactions using the pGFP-spl reporter. Samples of (A, B) HEK-293T and (C, D) MDA-MB-231 cell lines were analyzed. Cells were collected 1, 3 and 24 h after transfection using pGFP-spl and analyzed by RT-qPCR using primers for (A, C) mRNA and (B, D) pre-mRNA. In comparison to levels observed 1 h after transfection, fold change was calculated (y-axis). Statistical analysis was performed by One-way ANOVA with Tukey's post-hoc (GraphPad Prism 8.0.2). Only statistically significant differences are indicated. * $p < 0.01$; ** $p < 0.001$; *** $p < 0.0001$.

4. Limitations

Our work describes a new approach to visualize and quantify splicing reactions using cultured cells. Despite the ease of visualization using the fluorescence microscope, we consider extremely important that analyses are performed along with a negative control, to overcome possible background fluorescence intensities of different cells. In order to confirm different amounts of unspliced and spliced products, RT-qPCR should be performed with previously validated primers.

Availability of data and materials

The dataset used on this study are available from the corresponding author on reasonable request. Raw data is available at <https://github.com/PColtri/Menezes2025/>.

Funding

Fundação de Amparo à Pesquisa do Estado de São Paulo (FAPESP) grants 2017/06994–9, 2019/21874–5, 2023/02980–4 and Conselho Nacional de Desenvolvimento Científico e Tecnológico (CNPq) grant 474672/2013–1.

CRediT authorship contribution statement

Arthur T. Menezes: Writing – original draft, Visualization, Validation, Software, Methodology, Investigation, Formal analysis, Data curation, Conceptualization. **Helder Y. Nagasse:** Visualization, Validation, Software, Methodology, Investigation, Formal analysis, Data curation. **Hilan R. M. Lopes:** Visualization, Validation, Software,

Methodology, Investigation, Formal analysis, Data curation. **Patricia P. Coltri:** Writing – review & editing, Writing – original draft, Supervision, Resources, Project administration, Funding acquisition, Conceptualization.

Declaration of competing interest

The authors declare the following financial interests/personal relationships which may be considered as potential competing interests: Patricia Pereira Coltri reports financial support was provided by State of Sao Paulo Research Foundation. Patricia Pereira Coltri reports financial support was provided by National Council for Scientific and Technological Development. If there are other authors, they declare that they have no known competing financial interests or personal relationships that could have appeared to influence the work reported in this paper.

Acknowledgements

We are grateful to Gisela T. Ramos for excellent technical support. The authors also thank Melissa Jurica, Vanessa Freitas and Irene Yan for providing reagents.

Supplementary materials

Supplementary material associated with this article can be found, in the online version, at [doi:10.1016/j.btre.2025.e00887](https://doi.org/10.1016/j.btre.2025.e00887).

Data availability

Data will be made available on request.

References

- [1] Y. Lee, D.C. Rio, Mechanisms and regulation of alternative pre-mRNA splicing, *Annu. Rev. Biochem.* 84 (2015) 291–323.
- [2] M.E. Wilkinson, C. Charenton, K. Nagai, RNA splicing by the spliceosome, *Annu. Rev. Biochem.* 89 (2020) 359–388.
- [3] J.P. Staley, C. Guthrie, Mechanical devices of the spliceosome: motors, clocks, springs, and things, *Cell*. 92 (3) (1998) 315–326.
- [4] G.S. França, M.D. Vitrano, P.A. Galante, Host gene constraints and genomic context impact the expression and evolution of human microRNAs, *Nat. Commun.* 7 (2016) 11438.
- [5] P.P. Coltri, M.G.P. Dos Santos, G.H.G. da Silva, Splicing and cancer: challenges and opportunities, *Wiley. Interdiscip. Rev. RNA*. 10 (3) (2019) e1527.
- [6] T. Alpert, L. Herzel, K.M. Neugebauer, Perfect timing: splicing and transcription rates in living cells, *Wiley. Interdiscip. Rev. RNA*. 8 (2) (2017).
- [7] X. Shi, M. Won, C. Tang, Q. Ding, A. Sharma, F. Wang, J.S. Kim, RNA splicing based on reporter genes system: detection, imaging and applications, *Coord. Chem. Rev.* 477 (2023).
- [8] J. Xie, H. Zheng, S. Chen, X. Shi, W. Mao, F. Wang, Rational design of an activatable reporter for quantitative imaging of RNA aberrant splicing *In vivo*, *Mol. Ther. Methods Clin. Dev.* 17 (2020) 904–911.
- [9] A.A. Pai, F. Luca, Environmental influences on RNA processing: biochemical, molecular and genetic regulators of cellular response, *Wiley. Interdiscip. Rev. RNA*. 10 (1) (2019) e1503.
- [10] H. Zheng, S. Chen, X. Wang, J. Xie, J. Tian, F. Wang, Intron retained bioluminescence reporter for real-time imaging of pre-mRNA splicing in living subjects, *Anal. Chem.* 91 (19) (2019) 12392–12398.
- [11] A. Anna, G. Monika, Splicing mutations in human genetic disorders: examples, detection, and confirmation, *J. Appl. Genet.* 59 (3) (2018) 253–268.
- [12] S. Zheng, IRAS: high-throughput identification of novel alternative splicing regulators, *Methods Enzymol.* 572 (2016) 269–289.
- [13] R. Das, Z. Zhou, R. Reed, Functional association of U2 snRNP with the ATP-independent spliceosomal complex E, *Mol. Cell.* 5 (5) (2000) 779–787.
- [14] M.H. Shihan, S.G. Novo, S.J. Le Marchand, Y. Wang, M.K. Duncan, A simple method for quantitating confocal fluorescent images, *Biochem. Biophys. Rep.* 25 (2021) 100916.
- [15] K.J. Livak, T.D. Schmittgen, Analysis of relative gene expression data using real-time quantitative PCR and the 2(-Delta Delta C(T)) method, *Meth.* 25 (4) (2001) 402–408.
- [16] M. Chalfie, Y. Tu, G. Euskirchen, W.W. Ward, D.C. Prasher, Green fluorescent protein as a marker for gene expression, *Sci.* (1979) 263 (5148) (1994) 802–805.
- [17] J. Liu, Y. Wang, A.A. Szalay, A. Escher, Visualizing and quantifying protein secretion using a Renilla luciferase-GFP fusion protein, *Lumin.* 15 (1) (2000) 45–49.
- [18] S. Subramanian, F. Sreenc, Quantitative analysis of transient gene expression in mammalian cells using the green fluorescent protein, *J. Biotechnol.* 49 (1–3) (1996) 137–151.
- [19] O. Shaul, How introns enhance gene expression, *Int. J. Biochem. Cell Biol.* 91 (Pt B) (2017) 145–155.
- [20] C.L. Will, R. Luhrmann, Spliceosome structure and function, *Cold. Spring. Harb. Perspect. Biol.* 3 (7) (2011).
- [21] T.W. Nilsen, Preparation of nuclear extracts from HeLa cells, *Cold. Spring. Harb. Protoc.* 2013 (6) (2013) 579–583.
- [22] S. Chen, W. Shu, H. Zheng, Z. Ma, M. Li, F. Wang, Dynamic visualization of mRNA splicing variants with a transactivating reporter, *Chem. Commun. (Camb)* 57 (75) (2021) 9594–9597.
- [23] B. Guo, X. Shi, Z. Ma, M. Ji, C. Tang, F. Wang, A ratiometric dual luciferase reporter for quantitative monitoring of pre-mRNA splicing efficiency *in vivo*, *J. Biol. Chem.* 297 (2) (2021) 100933.
- [24] H.B. Schmidt, A. Barreau, R. Rohatgi, Phase separation-deficient TDP43 remains functional in splicing, *Nat. Commun.* 10 (1) (2019) 4890.
- [25] P. Stoilov, C.H. Lin, R. Damoiseaux, J. Nikolic, D.L. Black, A high-throughput screening strategy identifies cardiotonic steroids as alternative splicing modulators, *Proc. Natl. Acad. Sci. U S A* 105 (32) (2008) 11218–11223.
- [26] I. Younis, M. Berg, D. Kaida, K. Dittmar, C. Wang, G. Dreyfuss, Rapid-response splicing reporter screens identify differential regulators of constitutive and alternative splicing, *Mol. Cell Biol.* 30 (7) (2010) 1718–1728.
- [27] M. Stevens, E. Star, M. Lee, E. Innes, L. Li, E. Bowler, S. Harper, D.O. Bates, S. Oltean, The VEGF-A exon 8 splicing-sensitive fluorescent reporter mouse is a novel tool to assess the effects of splicing regulatory compounds *in vivo*, *RNA Biol.* 16 (12) (2019) 1672–1681.